Thermo-Hydraulic Performance Analysis of a Microchannel Flat-Tube Heat Exchanger with Finned Enhancements

Thanhtrung Dang
Department of Thermal Engineering, Ho Chi Minh City University of Technology and Education

Hoangtuan Nguyen
Department of Thermal Engineering, Ho Chi Minh City University of Technology and Education

Kyaw Thu
Department of Advanced Environmental Science and Engineering, Faculty of Engineering Sciences, Kyushu University

https://doi.org/10.5109/7363515

出版情報：Evergreen. 12 (2), pp.1380-1391, 2025-06. 九州大学グリーンテクノロジー研究教育センター
バージョン：

Thermo-Hydraulic Performance Analysis of a Microchannel Flat-Tube Heat Exchanger with Finned Enhancements

Thanhtrung Dang[1,*], Hoangtuan Nguyen[1], Kyaw Thu[2,3]

[1]Department of Thermal Engineering, Ho Chi Minh City University of Technology and Education, Ho Chi Minh City 71307, Viet Nam
[2]Department of Advanced Environmental Science and Engineering, Faculty of Engineering Sciences, Kyushu University, Kasuga-koen 6-1, Kasuga-city, Fukuoka 816-8580, Japan
[3]Research Center for Next Generation Refrigerant Properties (NEXT-RP), International Institute of Carbon-Neutral Energy Research (I2CNER), Kyushu University, 744 Motooka, Nishi-ku, Fukuoka 819-0395, Japan

*Author to whom correspondence should be addressed:
E-mail: trungdang@hcmute.edu.vn

(Received May 01, 2025; Revised June 10, 2025; Accepted June 11, 2025)

Abstract: The present study investigated the thermo-hydraulic characteristics in a microchannel heat exchanger that has a capacity of 2.6kW with the surface area of 2.5m2 configured with finned and microchannel flat tubes. The analysis covers both analytical and comprehensive experimental evaluations of the heat transfer characteristics and pressure drop phenomena. Two fluids (water and air) were assumed to have constant properties. Parameters such as the total pressure drop, the actual effectiveness, the NTU effectiveness, the rate of heat transfer, the heat flux, the log-mean temperature difference, the overall heat transfer coefficient, and the performance index were determined. At the inlet water temperature of 60°C, the actual effectiveness decreases from 90.5% to 74%; the NTU effectiveness decreases from 82.4% to 61.3%; the heat flux increases from 632.6 W/m2 to 943.9 W/m2; the log-mean temperature difference increases from 9oC to 10.3oC, calculating the overall heat transfer coefficient increases from 70.1 W/m2K to 92.1 W/m2K as rising the water velocity from 0.488 m/s to 0.975 m/s. In addition, two regression equations are proposed to determine the Poiseuille number in this study range. Furthermore, the analytical and experimental results are in good agreement.

Keywords: heat exchanger; heat transfer; microchannel; overall heat transfer coefficient; pressure drop

1. Introduction

The interest in microchannel technology has been gaining momentum. Microchannels are widely applied in heat exchangers because of their ability to enhance heat transfer efficiency and impair pressure drop. With a compact design and high efficiency, microchannels play a crucial role in cooling electronic devices, heating, drying, refrigeration, and modern industrial applications.

Manifold microchannel heat exchangers (MMC) offer high performance by improving temperature uniformity and significantly reducing pressure drop. Boteler et al.[1)] demonstrated that MMCs can decrease pressure drop up to 97% compared to the conventional straight microchannels due to the non-uniform flow distribution and vortex effects within the microchannels. Additionally, the optimization study of MMC design on the inlet to outlet manifold length ratio suggested that the highest heat transfer efficiency was achieved when the ratio was approximately three[2)]. Arie et al. proposed a multi-objective optimization method applied to MMCs based on two criteria: maximizing heat flux and minimizing pumping power, thereby enhancing the overall cooling system efficiency[3)]. The geometric design of heat sinks significantly influences the performance, with increasing in the number of channels from 100 to 143, reducing the pressure drop by 53.29% and improving heat transfer efficiency by 17.27%[4)]. Other studies[5-7)] have shown that the optimal solid material volume fraction ranges from 20% to 30% to balance heat transfer and pressure drop. Secondary channels and microstructures such as pillars or micropores can improve the heat transfer coefficient around 30%-50%, with micropores causing less pressure drop. Using rectangular channels with a 4:1 aspect ratio improves heat transfer by 15% compared to square channels.

Cite: T. Dang, H. Nguyen, K. Thu, "Thermo-Hydraulic Performance Analysis of a Microchannel Flat-Tube Heat Exchanger with Finned Enhancements". Evergreen, 12 (02) 1380-1391 (2025). https://doi.org/10.5109/7363515.

Research on manifold microchannel heat sinks (MMC) showed that they significantly reduce thermal resistance compared to traditional microchannels (TMC)[8]. The use of multiple inlet/outlet configurations enhanced cooling efficiency as well as temperature uniformity across the heat sink surface. Geometric parameters such as microchannel width, depth, and inlet/outlet channel widths have significant impacts on the performance. Experimental results indicated that MMCs can reduce thermal resistance by up to 35% compared to TMCs, demonstrating the effectiveness of this design. Some studies reported on the refrigerant flow patterns inside the wire-on-tube heat exchangers with varying low flow rates[9]. Several studies have been reported on thermodynamic analysis and channel geometry. For instance, Sharma et al. studied an MMC heat exchanger using hot water, revealing high thermodynamic efficiency due to the heat recovery capability from high-power electronic devices, thus improving the overall system efficiency[10,11].

MMCs have often been applied to liquid cooling applications. A novel MMC evaporator design was evaluated with refrigerant R-134a, that achieved a heat transfer coefficient above 10,000 W/m²K with a low pressure drop, highlighting its potential for absorption refrigeration systems. Additionally, research by Boyea et al. introduced an MMC condenser with microgrooves measuring 60 × 600 μm and demonstrated a heat transfer coefficient of up to 60 kW/m²K with only 7 kPa pressure drop, emphasizing the efficiency enhancement potential of MMCs[12]. Low pressure drops in MMC have been further supported by incorporating microgroove structures in MMCs enhances heat transfer without significantly increasing flow pressure[13].

Several studies have focused on the flow velocity in MMCs. In a tea-focused fluidized bed dryer, Yohana et al. numerically explored the effect of varying inlet air velocity on heat and mass transfer[14]. Afzal et al. demonstrated the decrease in the Nusselt number (alongside the channel length) due to thermal boundary layer effects[15], They further discussed the influence of varying Reynolds numbers (200 to 800) on the flow development region. Instabilities in microchannels include strong pressure oscillations and milder parallel-channel instabilities, which can lead to early onset of critical heat flux[16]. For two-phase pressure drop, a new correlation developed has an average error of only 8.2%, which is a significant improvement compared to previous methods[17]. On the other hand, the two-phase friction factor increases by 1.5 to 3 times compared to the single-phase flow, depending on the Reynolds number and vapor-liquid ratio[18]. Adding cavities to microchannels often enhances the heat transfer (up to 20% in some cases), while reducing pressure drop by approximately 15% when compared to straight channels. Hydraulic diameters from 60 μm to 2000 μm have been analyzed to assess the impact of geometry on heat transfer[19,20]. Zhou et al. designed a two-layer parallel microchannel heat exchanger, showing the optimal performance when the width is 0.4–0.6 mm, height 1–1.5 mm, and spacing 0.6–0.8 mm[21]. The Nusselt number enhances for increased width and decreased height, while the friction factor impairs as spacing increases. Additionally, numerous studies have expanded applications of MMCs in cooling and energy technologies. With the development of micro and nanoscale electronic devices, efficient thermal management has become critical, and MMCs are considered as promising solutions for high-power cooling and heating systems[22]. Studies on flow transitions in microchannels have shown shifts from laminar to turbulent flow. These advances are beneficial to the application of MMC designs for industrial applications[23-25].

Refrigerants exhibit different heat transfer efficiencies in multiport tubes[26-28]. However, these studies were performed for only elements and not the entire heat exchanger. Nanofluids containing copper or alumina nanoparticles increase the heat transfer coefficient by 15% to 40% compared to water, particularly in microchannels with inserts[28]. Kaushik et al. demonstrated that Ammonia exhibits a 20%-30% improved heat transfer coefficient than R-134a and R-22[29]. However, the improvement is subject to the optimization to offset greater entropy generation. Meanwhile, R-134a provides stable performance with lower pressure, making it suitable for energy saving systems[30].

Optimizing coolant selection significantly improves the heat transfer performance in microchannels. Studies on two-phase flow in microchannels often report an advanced heat flux than the single-phase flow, particularly at low Reynolds numbers[30,31]. Additionally, a study on TiO_2-water nanofluids showed that adding nanoparticles to the coolant enhances heat transfer up to 2.0%. Both studies emphasized the potential for reducing thermal resistance through flow characteristic adjustments and coolant selection.

Table 1: Summary of research data

Ref.	Material/ Shape	Working fluid	Flow rate	Heat transfer	Pressure drop	Comments
Boteler et al.[1]	Rectangular	Water	0.9 - 9 ml/m	21 kW/m²K	-	Modeling the entire manifold structure, detecting complex flow phenomena

Cite: T. Dang, H. Nguyen, K. Thu, "Thermo-Hydraulic Performance Analysis of a Microchannel Flat-Tube Heat Exchanger with Finned Enhancements". Evergreen, 12 (02) 1380-1391 (2025). https://doi.org/10.5109/7363515.

Sarangi et al.[2]	Rectangular	Water	0.5 - 1.5 g/s	29,12 kW/m²K	382 - 2283 Pa	Optimization Under Uncertainty, sensitivity analysis
Zhuan et al.[4]	Rectangular	Water two phase flow	u = 0.65 m/s	16.16 W/cm²K	-	Use multiphase flow VOF model
Shi et al.[5]	Rectangular	Deionized water	0.04 g/s	5 kW/m²K	14 kPa	Multi-objective optimization
Rajalingam and Chakraborty[6]	Triangle	Water	3 g/s	Nu = 26.55	-	Improve the heat transfer pressure drop by the micro blind holes
Mat et al.[7]	Rectangular	Water	4.6 cm³/s	-	60 kPa	CFD, RSM and NSGA2 algorithm
Kim et al.[8]	Rectangle with inside fin	Air	u = 0.0015 m³/s		400 Pa	Geometric optimisation
Mahdi et al.[9]	Circle	R-600a, R-134a	1- 5.5 kg/h	-	-	Investigate the flow patterns of refrigerant
Sharma et al.[10]	Rectangular	Hot water	From 0.3 to 1.0 l/m	-	-	Detailed analysis of thermo-hydrodynamics
Jha et al.[11]	Rectagngle with triangular minigrooves	Deionized water	100–600 ml/s	10 kW/m²K	100 mbars	Design, Fabrication and Experimental Testing
Boyea et al.[12]	Rectangular	R236fa, R134a	0.5679 kg/s	22 kW/m²K	7 kPa	Enhances heat transfer while minimizing pump capacity
Andhare et al.[13]	Rectangular	Water	20 g/s	20 kW/m²K	5.85 bar/m	Design, Fabrication and Testing
Husain et al.[15]	Rectangular	Water	-	-	-	Channel shape design and optimization
Bello-Ochende et al.[16]	Rectangular	Water	Re is from 200 to 800	-	10 - 75 kPa	Geometric optimisation
Tiselj et al.[17]	Isosceles triangle	Water	Re from 3.2 to 64	-	-	Experiments and 3D simulations
Kaushik et al.[18]	Rectangular strip	Hybrid nanofluid CuO+ZnO+H_2O	46.92 ml/m	16,836 kW/m²K	-	Experiments and CFD simulations
Huang et al.[19]	Triangle	Deionized water	0.96 ml/m	1.5 – 2.5 kW/m²K	5 kPa	Enhances heat transfer test analysis
Hetsroni et al.[20]	Circular, rectangular, trapezoida	Demineralized water	Re from 140 to 1400	25.905 kW/m²K	-	Comparing experimental results with theory
Zhou et al.[21]	Rectangular	Deionized water	100 - 900 ml/m	-	8,32 kPa	Experiments and CFD simulations
Naqiuddin et al.[22]	Wavy, Straight, Dimples channel	Deionized water	$100 \leq Re \leq 1000$	7.9 MW/m²K	-	Study in geometric design
Hetsroni et al.[23]	Circular, rectangle, triangular trapezoidal	Deionized water	10-30 m/s	-	-	Roughness Analysis, energy dissipation
Arie et al.[24]	Rectangular with fin inside	Water	0.1 kg/s	Nu from 34.6 to 210.7	66.09 kPa	Numerical model development and heat exchanger optimization

Cite: T. Dang, H. Nguyen, K. Thu, "Thermo-Hydraulic Performance Analysis of a Microchannel Flat-Tube Heat Exchanger with Finned Enhancements". Evergreen, 12 (02) 1380-1391 (2025). https://doi.org/10.5109/7363515.

Sakanova et al. [25]	wavy channel	Pure water, nano fluid	0.152 - 0.354 l/m	-	-	Improve the efficiency of wavy and nanofluid channel structures
Dai et al. [26]	Rectangular and circular	Ethanol	50< Re< 2500	Nu is from 2 to 8	Friction facotr f is from 0.03 to 0.12	Experimental and theoretical results
Kaew-On et al. [27]	Rectangular	R134a	Mass flux from 300 to 800 kg/m²s	From 4000 to 16000 W/m^{2}K	-	Experimental and predicted results
Vakili-Farahani et al. [28]	Rectangular	R245fa and R1234ze	Mass flux from 100 to 400 kg/m²s	From 1000 to 5000 W/m^{2}K	-	Experimental and predicted results
Syahrul et al. [29]	Rectangular strip micro inserts	Hybrid nanofluid Al_20_3, ZnO,	9.37 ml/m, 375.3 ml/m	8,120-120,44 W/m2.K	-	New design for channel
Kaushik et al. [30]	Rectangular	R717, R22, R134a	Mass flux from 250 to 450 kg/m²s	-	-	Entropy Generation Method of Two Phase Flow
Ariyo and Bello-Ochende[31]	Rectangular	Deionized water	Velocity from 0.1 to 4.5 m/s	1200 W/cm²	0 – 25 kPa	Minimization of thermal resistance
Manay and Sahin[32]	Rectangular	20% eg	0.028 - 0.084 kg/s	7931 W/m²·K	6 – 11 kPa	Experimental study of the effects of nanosolutions
Nguyen et al. [33]	Rectangular	Water	0.016 - 0.032 l/s	108 W/m²K	38.5 - 66.94 kPa	Testing of heat transfer properties and pressure losses
Dang et al. [34]	Rectangular	Deionized water	0.1773-0.3239 g/s	0.625 - 0.815 W/cm²·K	880 - 4400 Pa	Numerical simulations and experiments to analyze the heat transfer properties

From the literature reviews above and summary of research data as shown in Table 1, it can be stated that most studies focus on channel geometry and optimization of the operating conditions across different configurations. Despite extensive research on MMCs and nanofluids, few studies have experimentally validated finned microchannel flat-tube configurations under controlled water-air flow conditions. In particular, performance metrics like actual versus NTU effectiveness and the performance index remain underreported. Therefore, the objective of this study is to experimentally and analytically evaluate the thermal and hydraulic performance of a compact heat exchanger configured with finned and microchannel flat tubes. Key performance metrics including heat flux, pressure drop, actual and NTU-based effectiveness, overall heat transfer coefficient, and performance index are determined under varying water flow rates and temperatures. This work addresses the lack of experimental data for hybrid microchannel flat-tube configurations and proposes regression models for predicting Poiseuille number behavior. The findings aim to optimize compact heat exchanger design for water-air systems in applications such as electronics cooling and HVAC (Heating, Ventilation and Air-Conditioning). The results in this paper are new, deeper, and broader development of the author's own results[34].

2. Methodology

2.1. Experiment setup

The detailed descriptions of the heat exchanger are shown in Figure 1. This heat exchanger is finned and flat tube type with water in the tube side and air on the outside of the tube. The water passes through six passes, a total of 29 flat tubes are distributed 3-4-5-6-6-5 corresponding to the passes. Flat tube has 10 microchannels; each microchannel has dimensions of 1.2 mm × 0.6 mm (the width and the depth) [33]. The microchannel heat exchanger incorporates V-type fins with a 1.1 mm pitch and 100 μm thickness. Experimental performance evaluation was conducted using the custom heat transfer test setup illustrated in Figure 2. The experimental setup comprises three primary components: a mini boiler generating hot water, the microchannel heat exchanger (MHE) with its flat-tube configuration, and the interconnecting piping system. In

Cite: T. Dang, H. Nguyen, K. Thu, "Thermo-Hydraulic Performance Analysis of a Microchannel Flat-Tube Heat Exchanger with Finned Enhancements". Evergreen, 12 (02) 1380-1391 (2025). https://doi.org/10.5109/7363515.

operation, heated water from the boiler circulates through the piping network into the MHE's flat tubes; meanwhile, the outside air flows over the flat tubes. Temperature sensors and the pressure transducers have been installed at the inlet and outlet of the heat transfer fluids. The experimental data has been acquired using MX-100 (Yokogawa). Figure 3 shows the pictorial view of the experimental facility. The accuracy specifications and measurement ranges of all testing instruments are detailed in Table 2. In this research, the water flow meter displays the volumetric flow rate.

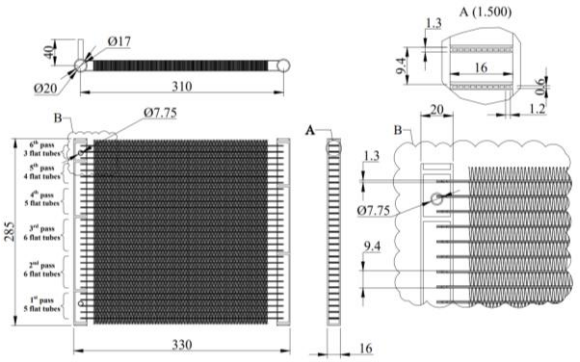

Fig. 1: Dimensions of the microchannel heat exchanger

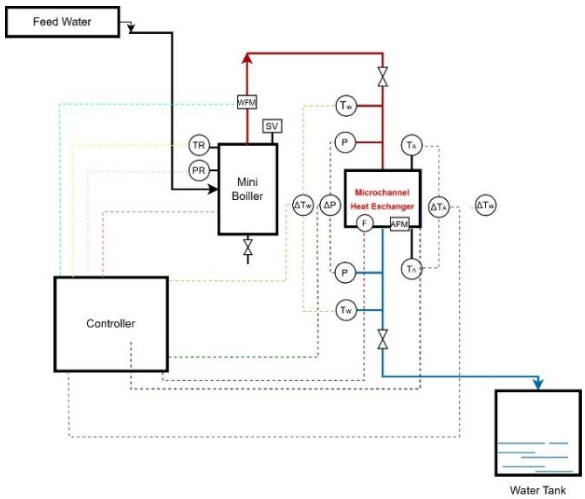

Fig. 2: The test rig for the heat exchanger

Table 2: Information on the instruments: Accuracies and ranges

Testing apparatuses	Accuracy	Range
Thermocouple, Type T, Omega, US	± 0.1°C	0 - 100°C
Pressure sensor Sensys, Korea	± 0.5 % FS	0 - 3 bar
Differential pressure transducer, GE Druck - UK	± 0.04 % FS	0 - 1 bar
Turbine flow meter Digital flow Co. LTD Korea	± 0.5 %	400 - 5000 l/h
Air flow meter Kimo Sauermann, France	±3 %	40 - 3500 m3/h

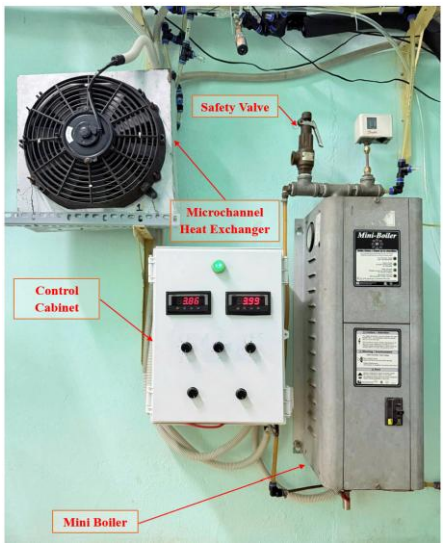

Fig. 3: The pictorial view of the experimental setup

2.2. Data reduction and models

This study investigates the thermal and heat transfer performance of a microchannel heat exchanger by analyzing key parameters: the heat transfer rate, heat flux, the actual effectiveness, the NTU (the number of transfer units) effectiveness, the pressure drop, the overall heat transfer coefficient, LMTD, and the performance index of a microchannel heat exchanger will be discussed.

In the range of this study, the specific heat of water and air remained almost constant. So, the heat transfer rates for both water and air sides are calculated as follows:

$$Q_w = m_w c_w (T_{w,i} - T_{w,0}) \quad (1)$$

$$Q_a = m_a c_a (T_{a,o} - T_{a,i}) \quad (2)$$

The maximum heat transfer rate:

$$Q_{max} = (mc)_{min} (T_{w,i} - T_{a,i}) \quad (3)$$

The actual effectiveness represents how efficiently a device transfers heat from the water side to the air side in real operating conditions. It is calculated by comparing the actual air-side heat gain to the maximum possible water-side heat transfer. It is determined by:

$$\varepsilon_a = \frac{Q_a}{Q_w} \quad (4)$$

The effectiveness by the NTU method is determined:

$$\varepsilon_{NTU} = \frac{Q_a}{Q_{max}} \quad (5)$$

The heat flux is calculated as below:

$$q = \frac{Q_a}{A} \quad (6)$$

The overall heat transfer coefficient is calculated as:

Cite: T. Dang, H. Nguyen, K. Thu, "Thermo-Hydraulic Performance Analysis of a Microchannel Flat-Tube Heat Exchanger with Finned Enhancements". Evergreen, 12 (02) 1380-1391 (2025). https://doi.org/10.5109/7363515.

$$U = \frac{q}{\Delta t_{lm}} \quad (7)$$

where: the subscript, *w*, is water and *a* is air. Here *Q* stands for the heat transfer rate (W), *m* is the mass flow rate (kg/s), *c* is the specific heat (kJ/kg.K), $T_{w,i}$ and $T_{w,o}$ are the temperatures of the inlet water and the outlet water (°C). Similarly, $T_{a,i}$ and $T_{a,o}$ are the temperatures of the inlet air and the outlet air (°C), *q* is the heat flux (W/m^2), *A* is the heat transfer area for the air side (m^2), *U* is the overall heat transfer coefficient (W/m^{2}K), and Δt_{lm} is the logarithmic mean temperature difference, (°C).

The total pressure drop of the water side is calculated as follows:

$$\Delta p = \Delta p_{fr} + \Delta p_l + \Delta p_{ac} + \Delta p_{gr} \quad (8)$$

where:

Δp_{fr}: Pressure drop by microchannel friction

Δp_l: Pressure drop by the entrance and exit of each channel

Δp_{ac}: Pressure drop by flow acceleration

Δp_{gr}: Pressure drop by gravitational force

With:

$$\Delta p_{fr} = \Delta p_{fr,cp1} + \Delta p_{fr,cp2} + \cdots + \Delta p_{fr,cpn} + \Delta p_{fr,m} \quad (9)$$

where:

$\Delta p_{fr,cp}$: Pressure drop by the microchannel friction of 1st, 2nd,..., nth pass.

$\Delta p_{fr,m}$: Pressure drop by the manifold friction.

The frictional pressure drop for each channel and manifold is determined by the expression:

$$\Delta p_{fr} = 2 f_F Re \frac{L}{{D_h}^2} w\mu \quad (10)$$

The Reynolds number is determined by:

$$Re = \frac{\rho w D_h}{\mu} \quad (11)$$

The total local pressure drop is determined:

$$\Delta p_l = \Delta p_{l,cp1} + \Delta p_{l,cp2} + \cdots + \Delta p_{l,cpn} \quad (12)$$

where:

$\Delta p_{l,cp}$: Local pressure drop by the entrance and exit of each channel of 1st, 2nd,..., nth pass

w: water velocity

f_F: Fanning friction factor.

Local pressure drop per channel is determined by:

$$\Delta p_{l,cp} = K_c \rho \frac{w^2}{2} + K_e \rho \frac{w^2}{2} \quad (13)$$

where:

K_c: Entrance loss coefficient

K_e: Exit loss coefficient.

The performance index serves as a quantitative measure of a heat exchanger's efficiency, reflecting its degree of thermal and hydraulic optimization. The higher this index, the greater the device capacity while the smaller the pressure drop.

The performance index ξ is calculated by:

$$\xi = \frac{Q_a}{\Delta p} \quad (14)$$

Based on relevant research as well as study limitations, a MHE with a capacity of 2.6 kW is designed and fabricated. Choosing the overall heat transfer coefficient U of 88.5 W/m2K and the log-mean temperature difference (tlm of 9.5 oC, the designed heat transfer area for air side is 2.5m2. (Figure 1).

3. Results and discussion

This study investigates the thermal and hydraulic performance of a microchannel heat exchanger (MHE) under controlled conditions. The water side was tested across five flow rates (0.016–0.032 l/s in 0.004 l/s increments) and five inlet temperatures (40–60°C in 5°C increments). For the air side, a constant flow rate of 190 l/s and an inlet temperature range of 30–31°C were maintained. Experimental measurements of temperature, pressure, and flow rates enabled the determination of key thermophysical properties, including density, specific heat, and dynamic viscosity. These parameters were subsequently used to calculate the water-side pressure drop in the MHE. In microchannels, the calculated Reynolds number for the water side ranges from 460.5 to 1867.7; thus, the flow inside the heat exchanger is laminar. In this study, the Poiseuille number (Po = fRe) is chosen from 15.5-20[35]; the entrance loss coefficient is taken as 0.8 and the exit loss coefficient is set as 1[36]. The total pressure drop of the MHE on the water side was evaluated for each channel/pass at a fixed inlet temperature of 50°C, as summarized in Table 3. The analysis revealed that the manifold's contribution to the pressure drop was negligible relative to the MHE's total pressure drop. Furthermore, local pressure losses at the entrance and exit regions accounted for approximately 3~9% of the total pressure drop.

Table 3: The total pressure drop of MHE by calculating each channel/pass

Parameters	Flow rate (l/s)				
	0.032	0.028	0.024	0.020	0.016
Velocity Pass_1 (m/s)	1.48	1.30	1.11	0.93	0.74
Frictional PD Pass_1 (kPa)	13.75	12.66	11.53	10.32	9.01
Entrance and exit PD Pass_1 (kPa)	1.96	1.50	1.10	0.77	0.49
Velocity Pass_2 (m/s)	1.11	0.97	0.83	0.69	0.56

Cite: T. Dang, H. Nguyen, K. Thu, "Thermo-Hydraulic Performance Analysis of a Microchannel Flat-Tube Heat Exchanger with Finned Enhancements". Evergreen, 12 (02) 1380-1391 (2025). https://doi.org/10.5109/7363515.

Frictional PD Pass_2 (kPa)	10.31	9.5	8.65	7.74	6.76
Entrance and exit PD Pass_2 (kPa)	1.10	0.84	0.62	0.43	0.28
Velocity Pass _3 (m/s)	0.89	0.78	0.67	0.56	0.44
Frictional PD Pass_3 (kPa)	8.25	7.60	6.92	6.20	5.41
Entrance and exit PD Pass_3 (kPa)	0.70	0.54	0.40	0.28	0.18
Velocity Pass _4 (m/s)	0.74	0.65	0.56	0.46	0.37
Frictional PD Pass_4 (kPa)	6.87	6.33	5.76	5.16	4.51
Entrance and exit PD Pass_4 (kPa)	0.49	0.37	0.28	0.19	0.12
Velocity in manifold (m/s)	0.14	0.12	0.11	0.09	0.07
Manifold PD (kPa)	0.005	0.005	0.004	0.003	0.003
Total PD (kPa)	59.97	54.18	48.60	42.92	36.97

(where PD is pressure drop)

The results in Table 2 were calculated with different number of flat tubes for each pass in 6 passes (3-4-5-6-6-5). To simplify the mathematical model, an approach is given that the 6 passes have the same number of flat tubes for each pass, corresponding to an average value of 4.83 flat tubes for each pass (29 flat tubes in total). Table 3 shows the calculated total pressure drops of MHE by calculating average velocity in microchannels/passes with the inlet water temperature of 50°C. From Table 2 and Table 3, it is observed that the total pressure drop between two calculation methods are the same. Thus, throughout the remainder of this study, the average water velocity is used to calculate and analyze the thermo-fluid phenomena of the MHE.

Table 3: The calculated total pressure drop of MHE by calculating average water velocity

Volumetric flow rate for water side, l/s	Average water velocity, m/s	Total pressure drop, (kPa)
0.032	0.975	59.98
0.028	0.853	54.18
0.024	0.731	48.60
0.020	0.610	42.92
0.016	0.488	36.97

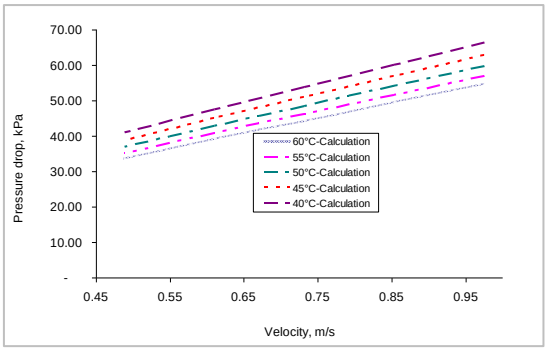

Fig. 4: The calculated total pressure drops in the water side for various flow velocities

The total pressure drop on the water side was calculated for different inlet temperatures, as illustrated in Figure 4. When the water velocity increased from 0.488 m/s to 0.975 m/s, the pressure drop rose from 33.79 kPa to 54.82 kPa at an inlet temperature of 60°C. Experimental measurements of the pressure drop, presented in Figure 5, further confirmed this trend. Additionally, the results indicated that the pressure drop decreased with rising temperature, attributed to the reduction in dynamic viscosity. These findings align with previously reported data in the literature[34,36].

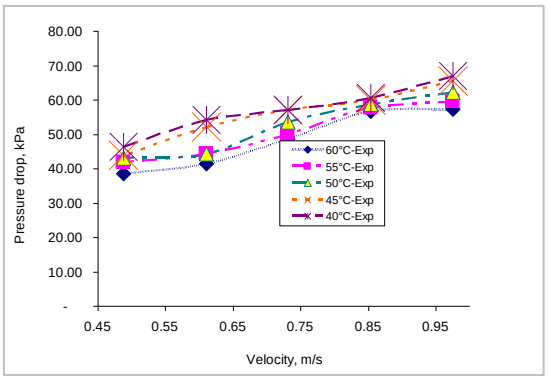

Fig. 5: Experimental results of the total pressure drop for the water side

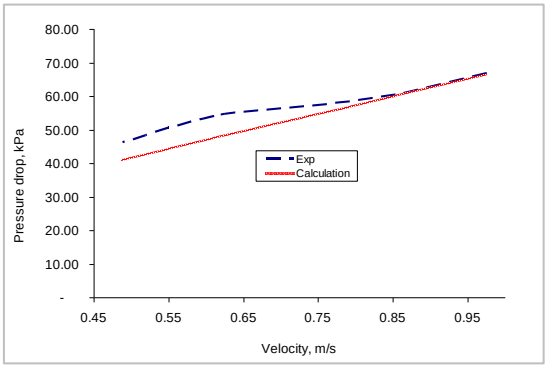

a) For the inlet water temperature of 40°C

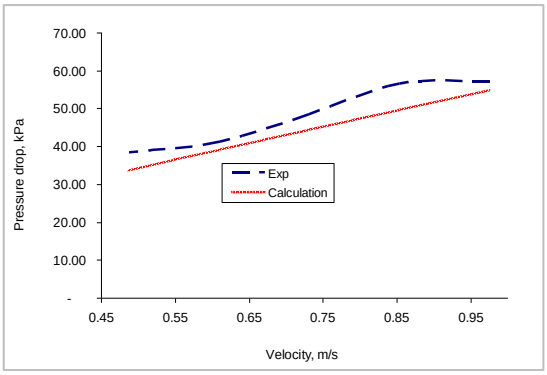

b) The inlet water temperature of 60°C

Fig. 6: Comparison between calculations and experimental results for the pressure drops

Figure 6 shows a comparison of the analytical and experimental results, for two sets of inlet water temperatures. From Figs. 4-6, the analytical and experimental results are in good agreement, with percentage errors of less than 20%. This deviation may be due to the experimental error. However, this value is still within the allowable error when comparing theory and experiment in thermofluids (maximum 30%).

The heat transfer rates of MHE for both sides of the fluids are shown in Figure 7. Within the range of this study, the heat transfer rate increases with increasing the water velocity and inlet water temperature. The highest capacities of MHE for water side and air side are 3.19 kW and 2.36 kW with water temperature of 60°C at the inlet, respectively.

When the water velocity increases, the heat transfer rate for water side increases more strongly than that gained from the heat transfer rate for air side. This leads to a decrease of effectiveness as increasing the water velocity, as shown in Figure 8. It is observed that the actual effectiveness value is higher than the NTU effectiveness value at the same water velocity. With the inlet water temperature of 60°C, as the water velocity increases from 0.488 m/s to 0.975 m/s, the actual effectiveness decreases from 90.5% to 74%; meanwhile, the NTU effectiveness decreases from 82.4% to 61.3%.

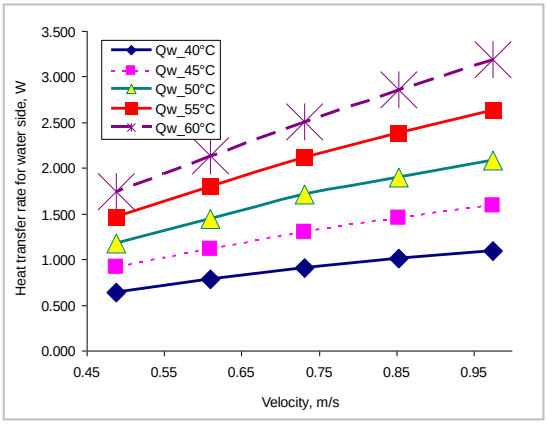

a) For water side

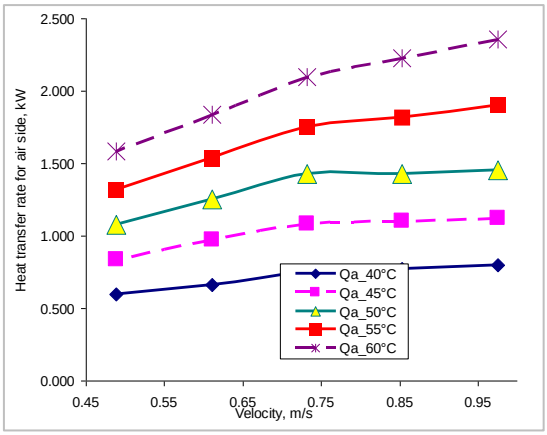

b) For air side

Fig. 7: Heat transfer rate vs. water velocity

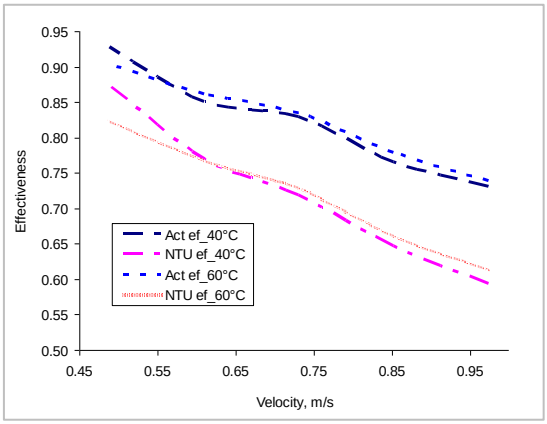

Fig. 8: Effectiveness vs. water velocity

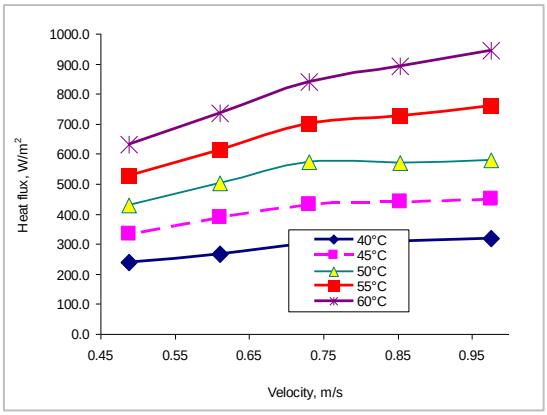

Fig. 9: Heat flux vs. water velocity

As the water velocity increases, the heat transfer rate for the water side becomes higher, increasing the heat transfer rate for the air side, which leads to a rise in heat flux, as shown in Figure 9. It is noted that the heat flux calculated for the air side. This trend is the same as the heat transfer rate for air side by the constant heat transfer area. The maximum heat flux is achieved at a 60°C inlet water temperature. As shown in Figure 10, when the water velocity increases from 0.488 m/s to 0.975 m/s under these conditions, the heat flux rises from 632.6 to 943.9 W/m²,

Cite: T. Dang, H. Nguyen, K. Thu, "Thermo-Hydraulic Performance Analysis of a Microchannel Flat-Tube Heat Exchanger with Finned Enhancements". Evergreen, 12 (02) 1380-1391 (2025). https://doi.org/10.5109/7363515.

the LMTD increases from 9.0 to 10.3°C, and the overall heat transfer coefficient improves from 70.1 to 92.1 W/m²·K. The results are consistent with the analytical data in Section 2.1. The experimental results in Figs. 9 and 10 are useful for the design of finned and flat tube type MHEs. The performance index for water side of the MHE tends to increase with increasing water velocity, as shown in Figure 11, the highest performance index is achieved at an inlet water temperature of 60°C. Under these conditions, the performance index increases from 45.4 W/kPa to 55.6 W/kPa as the water velocity rises from 0.488 m/s to 0.975 m/s.

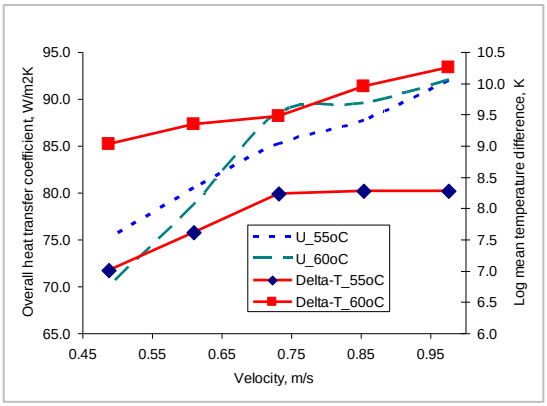

Fig. 10: Overall heat transfer coefficient vs. water velocity

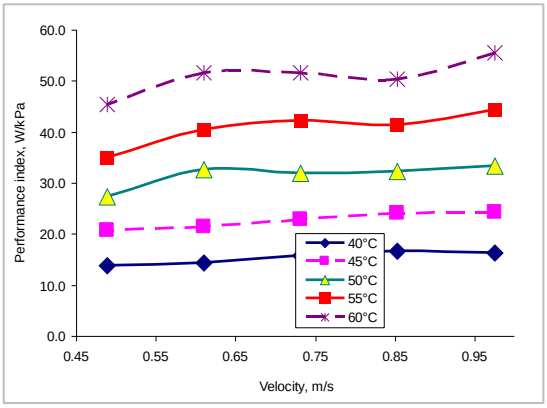

Fig. 11: Performance index vs. water velocity

From many experiments for this MHE, the analytical results for the total pressure drop are always much lower than the experimental results when keeping the Poiseuille number constant. The deviation is obvious at low water velocities. Two regression equations are proposed to determine the Poiseuille number in the study range. When applying these equations with the water velocity from 0.488 m/s to 0.975 m/s, the experimental and theoretical analysis results are in good conformity.

The Poiseuille number versus the water velocity w:

$$Po = 15.084w^{-0.3713}$$

The Poiseuille number versus the water flow rate V:

$$Po = 4.2517V^{-0.3707}$$

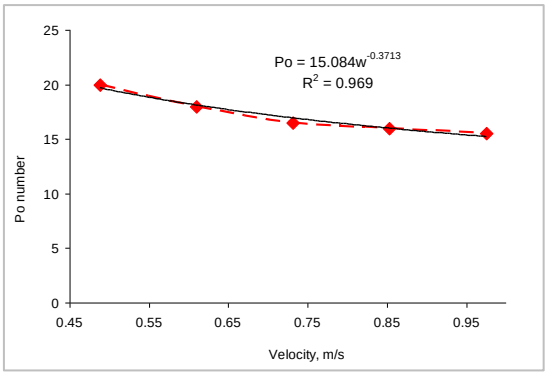

Fig. 12: Experimental results for Po number

In summary, the key parameters investigated in this study - including heat flux, overall heat transfer coefficient, performance index, and pressure drop components (both frictional and local) - provide essential data for optimizing the design of finned-tube and microchannel flat-tube heat exchangers. The high-performance index and low manifold losses suggest this MHE design is well-suited for applications like HVAC heat recovery systems and compact data center cooling units.

4. Conclusions

In this study, thermo-fluid behaviors in a heat exchanger (finned and microchannel flat tube) have been investigated both analytically and experimentally. This MHE has the designed capacity of 2.6 kW and the heat transfer area for air side of 2.5m^2. For the air side, the flow rate was fixed at 190 l/s and the inlet temperature was around 30 – 31°C. On the water side, experiments were conducted under five controlled flow rates and five inlet temperature conditions. As the water velocity increased from 0.488 m/s to 0.975 m/s, the principal findings of this study were as follows:

- The total pressure drop for water side by calculating average velocity in microchannels/passes is the same as calculating different number of flat tubes for each pass in six passes.
- The pressure drop of the manifold is negligible relative to the total pressure drop, with local entrance/exit losses accounting for approximately 3~9% of the total pressure drop.
- With the inlet water temperature of 60°C, the actual effectiveness decreases from 90.5% to 74%; meanwhile, the NTU effectiveness decreases from 82.4% to 61.3%.
- At an inlet water temperature of 60°C, the heat flux rises from 632.6 W/m² to 943.9 W/m², while the LMTD increases from 9°C to 10.3°C. Consequently, the calculated overall heat transfer coefficient increases from 70.1 W/m²·K to 92.1 W/m²·K.
- When the water enters at 60°C, the performance index goes up from 45.4 W/kPa to 55.6 W/kPa.
- Two regression equations are proposed to determine the Poiseuille number in study range.
- With percentage errors of less than 20%, the analytical

Cite: T. Dang, H. Nguyen, K. Thu, "Thermo-Hydraulic Performance Analysis of a Microchannel Flat-Tube Heat Exchanger with Finned Enhancements". Evergreen, 12 (02) 1380-1391 (2025). https://doi.org/10.5109/7363515.

and experimental results are in good similarity.
The current study assumes constant fluid properties; future work should integrate temperature-dependent property models and explore two-phase flow conditions for further design optimization.

Acknowledgements

This work is sponsored by the Ho Chi Minh City University of Technology and Education (HCMUTE), Vietnam. The supports (by project No. T2024-45) are deeply appreciated.

Nomenclature

m	mass flow rate ($kg \cdot s^{-1}$),
V	volumetric flow rate ($m^3 \cdot s^{-1}$),
c	specific heat ($kJ \cdot kg^{-1} \cdot K^{-1}$),
t	temperatures (°C),
q	heat flux ($W \cdot m^{-2}$),
f_F	Fanning friction factor
v	fluid velocity ($m \cdot s^{-1}$),
L	channel length (m)
D_h	hydraulic diameter (m)
Wc	microchannel width (m)
U	overall heat transfer coefficient ($W.m^{-2}K^{-1}$)
Δt_{lm}	Log-mean temperature difference (°C)
A	heat transfer area for air side (m^2)

Greek symbols

ε	effectiveness,
ρ	density ($kg \cdot m^{-3}$),
μ	dynamic viscosity ($kg/(m \cdot s^{-1})$),

Subscripts

w	Water side
a	Air side
in	inlet
o	outlet

References

1) L. Boteler, N. Jankowski, P. McCluskey, and B. Morgan, “Numerical investigation and sen-sitivity analysis of manifold microchannel coolers,” International Journal of Heat and Mass Transfer., 55 (25-26), 7698-7708 (2012). doi.org/10.1016/j.ijheatmasstransfer.2012.07.073
2) S. Sarangi, K. K. Bodla, S. V. Garimella, and J. Y. Murthy, “Manifold microchannel heat sink design using optimization under uncertainty,” International Journal of Heat and Mass Transfer., 69, 92-105 (2014). doi.org/10.1016/j.ijheatmasstransfer.2013.09.067
3) M. A. Arie, A.H. Shooshtari, S.V. Dessiatoun, M.M. Ohadi, and E. A. Hajri, “Simulation and Thermal Optimization of a Manifold Microchannel Flat Plate Heat Exchanger”, The American Society of Mechanical Engineers., 209-220 (2012). doi.org/10.1115/IMECE2012-88181.
4) R. Zhuan, W. Wang, “Simulation on nucleate boiling in micro-channel”, International Journal of Heat and Mass Transfer., 53 (1-3) 502-512 (2010). doi.org/10.1016/j.ijheatmasstransfer.2009.08.019.
5) X.Shi, S. Li , Y. Mu , B. Yin, “Geometry parameters optimization for a microchannel heat sink with secondary flow channel”, International Communications in Heat and Mass Transfer., 104, 89-100 (2019). doi.org/10.1016/j.icheatmasstransfer.2019.03.009
6) A.Rajalingam and S. Chakraborty, “Effect of micro-structures in a microchannel heat sink – A comprehensive study”, International Journal of Heat and Mass Transfer., 154, 851-862 (2020). doi.org/10.1016/j.ijheatmasstransfer.2020.119617
7) N.M. N. H. Mat, N.N. Mohd-Ghazali, N.H.S. Shamsuddin, and N.P.P Estellé, “Optimization of Microchannel Heat Sink for Thermal Performance and Pressure Drop using Central Composite Design of Experiment”. Evergreen, 11 (2) 1426–1434 (2024). doi.org/10.5109/7183463.
8) Y. H. Kim, W. C. Chun, J. T. Kim, B. C. Pak, and B. J. Baek, “Forced air cooling by using manifold microchannel heat sinks,” KSME International Journal., 12, 709-718 (1998). doi.org/10.1007/BF02945732.
9) L. A. A. Mahdi, M.A. Fayad, T. M. Chaichan, “Flow Patterns in Wire-on-Tube Heat Exchangers Based on Various Low Refrigerant Mass Flow Rates”, Evergreen, 11 (02) 872-886 (2024).
10) C.S. Sharma, M. K. Tiwari, B. Michel, and D. Poulikakos, “Thermofluidics and energetics of a manifold microchannel heat sink for electronics with recovered hot water as working fluid”, International Journal of Heat and Mass Transfer., 58, 135-151 (2013). doi.org/10.1016/j.ijheatmasstransfer.2012.11.012
11) V.Jha, S. Dessiatoun, A. Shooshtari, E. S. Al-hajri, and M. M. Ohadi, “Experimental Char-acterization of a Nickel Alloy-Based Manifold-Microgroove Evaporator,” Heat Transfer Engineering, 36 (1) 33-42 (2014). doi.org/10.1080/01457632.2014.906276.
12) D.Boyea, A.H. Shooshtari, S.V. Dessiatoun, and M.M. Ohadi, “Heat Transfer and Pressure Drop Characteristics of a Liquid Cooled Manifold-Microgroove Condenser, ASME Pro-ceedings”, The American Society of Mechanical Engineers., (2013). doi.org/10.1115/HT2013-17781.
13) R.S. Andhare, A. Shooshtari, S. V. Dessiatoun, and M. M. Ohadi, “Heat transfer and pres-sure drop characteristics of a flat plate manifold microchannel heat exchanger in counter flow configuration,”,

Applied Thermal Engineering., 96, 178-189 (2016). doi.org/10.1016/j.applthermaleng.2015.10.133.

14) E. Yohana, M. Tauviqirrahman, Y. L. Hakim, M. E. Yulianto, Ridho, M. F. H. Dwinanda, K.H Choi, "Exploring the Impact of Inlet Air Velocity Variations on Heat and Mass Transfer in a Tea-Focused Fluidized Bed Dryer: A Comprehensive Numerical Analysis", Evergreen, 11 (03) 2175-2185 (2024).
15) A.Husain, K.Y. Kim, "Shape Optimization of Micro-Channel Heat Sink for Micro-Electronic Cooling", IEEE Transactions on Components and Packaging Technologies., 31 (2) 322-330 (2008). doi: 10.1109/TCAPT.2008.916791.
16) T.Bello-Ochende , L. Liebenberg , J.P. Meyer, "Constructal cooling channels for micro-channel heat sinks", International Journal of Heat and Mass Transfer., 50 (21-22) 4141-4150 (2007). doi.org/10.1016/j.ijheatmasstransfer.2007.02.019.
17) I.Tiselj, G. Hetsroni, B. Mavko, A. Mosyak, E. Pogrebnyak, Z. Segal, "Effect of axial conduction on the heat transfer in micro-channels", International Journal of Heat and Mass Transfer., 47 (12-13) 2551-2565 (2004). doi.org/10.1016/j.ijheatmasstransfer.2004.01.008.
18) S.Kaushik, V. Uniyal, N. Verma, S. Joshi, M. Makhloga, N. P. S. Pargai, N. S. K. Sharma, R. Kumar, and S. Pal, (2023). "Comparative Experimental and CFD Analysis of Fluid Flow Attributes in Mini Channel with Hybrid CuO+ZnO+H_2O Nano Fluid and (H_2O) Base Fluid", Evergreen, 10 (1) 182–195 (2023). doi.org/10.5109/6781069.
19) B.Huang, H. Li, S. Xia, and T. Xu, "Experimental investigation of the flow and heat trans-fer performance in micro-channel heat exchangers with cavities", International Journal of Heat and Mass Transfer., 159 120575 (2020). doi.org/10.1016/j.ijheatmasstransfer.2020.120075.
20) G.Hetsroni , A. Mosyak , E. Pogrebnyak , L.P. Yarin, "Heat transfer in micro-channels: Comparison of experiments with theory and numerical results", International Journal of Heat and Mass Transfer., 48 (25-26) 5580-5601 (2005). doi.org/10.1016/j.ijheatmasstransfer.2005.05.041.
21) F.Zhou, W. Zhou, Q. Qiu, W. Yu, and X. Chu, "Investigation of fluid flow and heat trans-fer characteristics of parallel flow double-layer microchannel heat exchanger," Applied Thermal Engineering., 137, 616-631 (2018). doi.org/10.1016/j.applthermaleng.2018.03.069.
22) N.H.Naqiuddin, L.H. Saw, M.C. Yew, F. Yusof, T.C Ng, and M.K. Yew, "Overview of micro-channel design for high heat flux application", Renewable and Sustainable Energy Reviews., 82, 901-914 (2018). doi.org/10.1016/j.rser.2017.09.110.
23) G.Hetsroni , A. Mosyak , E. Pogrebnyak , L.P. Yarin, " Fluid flow in micro-channels", International Journal of Heat and Mass Transfer., 48 (10) 1982-1998 (2005). doi.org/10.1016/j.ijheatmasstransfer.2004.12.019.
24) M. A. Arie, A. H. Shooshtari, S. V. Dessiatoun, E. Al-Hajri, and M. M. Ohadi, "Numerical modeling and thermal optimization of a single-phase flow manifold-microchannel plate heat exchanger,", International Journal of Heat and Mass Transfer., 81 478-489 (2015). doi.org/10.1016/j.ijheatmasstransfer.2014.10.022.
25) A. Sakanova, C. C. Keian, and J. Zhao, "Performance improvements of microchannel heat sink using wavy channel and nanofluids," International Journal of Heat and Mass Transfer., 89, 59-79 (2015).
26) B.Dai, M. Li, C. Dang, Y. Ma, Q. Chen, "Investigation on convective heat transfer characteristics of singe phase liquid flow in multi-port micro-channel tubes", International Journal of Heat and Mass Transfer, 70 114–118 (2014) doi: //doi.org/10.1016/j.ijheatmasstransfer.2013.10.048
27) J.Kaew-On, K. Sakamatapan, S. Wongwises, "Flow boiling heat transfer of R134a in the multiport minichannel heat exchangers", Experimental Thermal and Fluid Science 35 364–374 (2011), doi:10.1016/j.expthermflusci.2010.10.007
28) F.Vakili-Farahani, B. Agostini, J.R. Thome, "Experimental study on flow boiling heat transfer of multiport tubes with R245fa and R1234ze(E)", International Journal of Refrigeration 36 (2) 335-352 (2013), doi: 10.1016/j.ijrefrig.2012.12.007
29) A.S.Syahrul, M. Normah, J. Oh, A. Robiah, and M. Yushazaziah, "Entropy Generation Minimization of Two-Phase Flow in a Mini Channel with Genetic Algorithm". Evergreen, 6 (1) 39-43 (2019). doi.org/10.5109/2321004.
30) S.Kaushik, N.K. Verma, S. Singh, N. Kanojia, S. Panwar, S. Kindo, S. Uniyal, S. Goswami, D. Som, and N.N.K. Yadav, (2023b). "Comparative Analysis of Fluid Flow Attributes in Rectangular Shape Micro Channel having External Rectangular Inserts with Hybrid Al_2O_3+ZnO+H_2O Nano Fluid and (H_2O) Base Fluid", Evergreen, 10 (2) 851-862 (2023). https://doi.org/10.5109/6792839.
31) D.O. Ariyo and T. Bello-Ochende, "Constructal design of subcooled microchannel heat ex-changers", International Journal of Heat and Mass Transfer., 146 (2020). doi.org/10.1016/j.ijheatmasstransfer.2019.118835
32) E. Manay and B. Sahin, "Heat Transfer and Pressure Drop of Nanofluids in a Microchannel Heat Sink", Nanomaterials, 38 (5) 510–522 (2016). doi.org/10.3390/nano9091231.

Cite: T. Dang, H. Nguyen, K. Thu, "Thermo-Hydraulic Performance Analysis of a Microchannel Flat-Tube Heat Exchanger with Finned Enhancements". Evergreen, 12 (02) 1380-1391 (2025). https://doi.org/10.5109/7363515.

33) B.N. Nguyen, T.T. Dang, H.T. Nguyen, T.H. Nguyen, and R. Munsin, Experimental Study on Heat Transfer Characteristics and Pressure Drop of a Fin and Microchannel Flat-Tube Heat Exchanger, Proceedings of GTSD2024, "Computational Intelligence Methods for Green Technology and Sustainable Development", Springer Science and Business Media LLC, 2024.
34) T.T. Dang, J.T. Teng, and J.C. Chu, "A study on the simulation and experiment of a microchannel counter-flow heat exchanger", Applied Thermal Engineering, 30 (14-15) 2163-2172 (2010).
35) S. G. Kandlikar, D.Q. Li, M. R. King, S. Garimella, S. Colin, "Heat transfer and fluid flow in minichannels and microchannels", Elsevier (2006).
36) W. M. Kays and A. L. London, "Compact Heat Exchangers", Third Edition, MEDTECH (2018).

Cite: T. Dang, H. Nguyen, K. Thu, "Thermo-Hydraulic Performance Analysis of a Microchannel Flat-Tube Heat Exchanger with Finned Enhancements". Evergreen, 12 (02) 1380-1391 (2025). https://doi.org/10.5109/7363515.